445. Investigation of Thermo-Elastic Damping of Vibrations of Rectangular and Ring-Shaped MEMS Resonators

R. Barauskas[1,a], S. Kausinis[1,b], H. A. C. Tilmans[2]
[1] Kaunas University of Technology, Studentu 50-407, LT-51368, Kaunas, Lithuania
[2] Interuniversity Microelectronics Center, Kapeldreef 75, B-3001, Leuven, Belgium,
e-mail: [a] *rimantas.barauskas@ktu.lt;* [b] *saulius.kausinis@ktu.lt;* [1] *Harrie.Tilmans@imec.be*

(Received 10 January 2009; accepted 10 March 2009)

Abstract. The paper deals with finite element analysis of damped modal vibrations Q-factor values determined by taking into account the thermally-elastic damping. Modal properties of square- and ring-shaped MEMS resonators have been investigated by taking into account the layered structure of MEMS and the influence of the geometry of the clamping zone. The calculations have been performed by employing the COMSOL Multiphysics finite element software. The solution method has been verified comparing numerically and analitically obtained damped modal properties of cantilever MEMS resonator. Experimental investigations of Q-factor values have been performed. The comparison of calculated and experimentally obtained resonant frequencies and Q-factor values indicated good agreement of tendencies of change of the quantities against temperature.

Keywords: thermally-elastic damping, finite elements, MEMS, resonator

1. Introduction

The scope of MEMS is expanding rapidly. Besides traditional MEMS, many new frontiers of practice were opened up in recent years, [1]. The most advanced solutions in terms of MEMS sensors, actuators, mechanical filters or microfluidic systems can be identified in inertial navigation systems, computer devices, industrial process control, electronics instrumentation, telecommunications as well as in biological and medical applications. Advanced MEMS applications are driven by processes that enable greater functionality and operational capabilities through higher levels of electronic-mechanical integration and greater numbers of mechanical components working either alone or together to enable a complex action.

To achieve these goals, the ways are being explored for reducing the power dissipation of both mechanical microstructures and electronical components by using innovative combinations of low-power circuits and micromechanical devices, [2]. A number of scientific and engineering challenges must be overcome in order to realize the vision for nano-micro-macro integration. Along with the development of new technologies, new device configurations and new applications for micro-sensors, micro-actuators and micro-systems, a growing need for achievement of better MEMS performance and for novel sensing capabilities can be observed.

In many applications, the benefits of using resonator microstructures relate directly to small size, high frequency and spectral purity. The latter quantity is defined by high values of the mechanical Q-factor. The damping rate of the vibrations can be evaluated as Q^{-1}, which is the rate at which energy of resonant vibrations is being lost to various environments coupled to the

model. The vibrations of real resonator structures are affected by several different energy loss mechanisms, which predetermine the overall value of the Q-factor. Unfortunately, the physical mechanisms of dissipation affecting the Q-factor values of micro-resonators are still not completely understood. It appears as very important to study different energy loss mechanisms and to perceive the dominating energy dissipation processes. Several studies, [3-10], have examined the different dissipation mechanisms, as well as, the dependence of the Q-factor on various parameters in both flexural and longitudinal vibration modes of MEMS structures. In particular, the Q-factor determined by thermal-elastic damping (TED) of micro-electro-mechanical resonators structures is a very important dynamic characteristic since it provides the upper limit of the Q-factor that is possible to achieve in a structure of a given geometry and materials under an assumption that no internal friction and other sources of damping are present.

In [4] the TED of the single-crystal 3C-SiC UHF nano-mechanical rod resonators at longitudinal vibration mode have been investigated and Q-factor values caused by TED at the thermal insulation boundary conditions, as well as, for the fixed temperature boundary conditions determined. The results have been employed for development and verification of FEM computational models in [3].

In [5] an extensive study of vibration energy loss mechanisms, which limit the highest achievable Q-factor values, has been presented. The damping mechanisms are predetermined by material properties and are highly influenced by the design of the resonator structures. They include energy losses mechanisms due to support clamping, air damping, heating, TED dissipation, anharmonic mode coupling, surface roughness, extrinsic noise, dislocations and dissipation due to two-level systems. Dependence of dissipation on the finite size of the structure, temperature, surface-aggregated defects, magnetic field, hysteresis and other factors has been analyzed. The data on dissipation measurements have been presented for micron-sized single crystal GaAs and Si resonators.

In [6] intrinsic and extrinsic energy loss mechanisms have been discussed and dissipation in polycrystalline diamond (poly-C) resonators has been explored by using electrostatic and piezoelectric actuation methods. Due to material limitations of poly-Si resonators, polycrystalline diamond (poly-C) has been explored as a new MEMS resonator material. The poly-C resonators were designed, fabricated and tested.

An effort to delineate the microscopic mechanisms predominantly responsible for dissipation in micromechanical resonators has been presented in [7]. Possible mechanisms contributing to dissipation in a double-clamped beam ultra-high frequency (UHF) nano-resonators have been analyzed in [8]. Estimation of the dissipation contributed by the evaporated metallic layers (Al and Ti) with internal friction has been presented in [9].

Although numerous approaches to the damping theory and experiments have been systematically developed and reported over several decades, advanced simulation and modelling tools are still needed in order to provide „advisory service“ at early stages of MEMS design. The numerical simulation is important for two reasons. First, it can be used to verify the analytical results, which often are obtained on the base of highly simplified models and then further used in order to explain similar phenomena in more complex MEMS configurations as well. The same model investigated numerically and analytically provides the base for the verification of the numerical model. Second, for complex geometry and multiple materials there are no analytical approximations, therefore numerical simulation is necessary.

This work presents the study of TED as a dissipation mechanism in modal damping of vibrations of rectangular- and ring-shaped MEMS resonators. Much of the work presented is numerical experiments has been performed to determining resonant frequencies and Q-factors of MEMS and providing physical interpretations of the results obtained. In addition, several real

physical experiments have been carried out, which demonstrated the reasonable agreement of computationally determined features to the reality.

2. FEM analysis of rectangular and ring-shaped resonators

A 3D computational model has been developed, which provides an approximation of the TED of structural vibrations of rectangular- and ring-shaped MEMS resonators. The model is based on the theoretical consideration developed in [3]. The layouts of two types of resonators are presented in Fig. 1 and Fig. 3. The model in COMSOL Multiphysics environment has been created as a coupled two-field Multiphysics problem.
Two application modes have been coupled:

- MEMS Module-> Structural Mechanics->Plane Stress->Damped eigenfrequency analysis
- COMSOL Multiphysics->Heat Transfer ->Conduction->Transient analysis.

The thermal-mechanical coupling has been ensured by entering the body heat source, which described the generation of the heat in the volume at given strain rates as $-\frac{T_0 \kappa c}{1-2\vartheta}\left(\frac{\partial \dot{u}}{\partial x}+\frac{\partial \dot{v}}{\partial y}+\frac{\partial \dot{w}}{\partial z}\right)$, and the thermal expansion strain $\kappa\left(T-T_0\right)$, which was taken into account in the mechanical equations of the model. Here $u(x,y,z)$, $v(x,y,z)$, $w(x,y,z)$ are displacements of the MEMS resonator structure at location $\left(x,y,z\right)$, c - Young's modulus, ϑ - Poisson's ratio, κ - thermal expansion coefficient, T_0 - ambient temperature.

The model is able to take into account the TED effect and the influence of the geometry of the clamping zone. Symmetric modes of rectangular- and ring-shaped resonators have been calculated by using quarter-symmetry models, Fig. 2 and Fig. 4. The mechanically free surfaces of the resonator are assumed to be thermally isolated basing on the fact that the heat exchange rate through the surface is too slow to be comparable with quick internal processes of acquiring and loosing heat caused by high rates of elastic strain. On the contrary, fixed temperature boundary conditions as $T=T_0$ have been imposed on cut boundaries, which represent the contact of the resonator with the overall MEMS structure.

Several in-plane (Figs.3-6 and Figs.13-16) and out-of-plane (Figs.7-10 and Figs.17-20) quarter-symmetry modal shapes are presented.

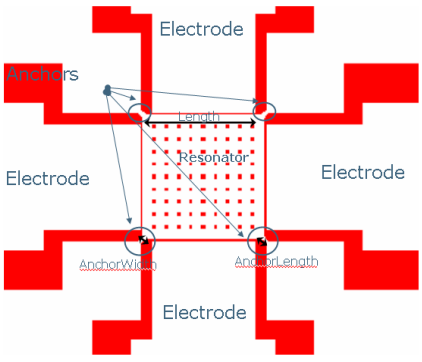

Fig. 1. The layout of the rectangular resonator

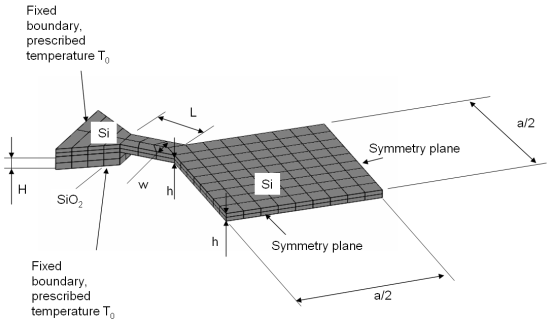

Fig. 2. The quarter symmetry model of the rectangular resonator

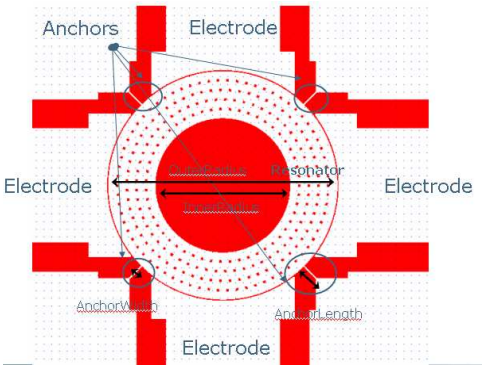

Fig. 3. The layout of the ring-shaped resonator

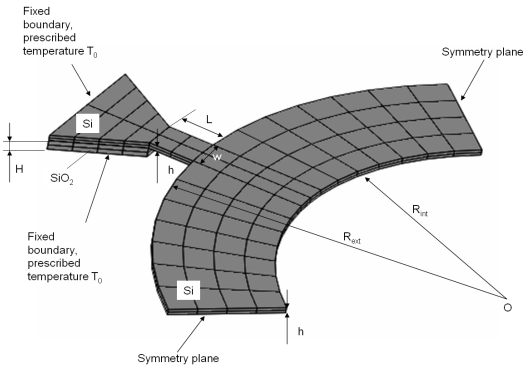

Fig. 4. The quarter symmetry model of the ring-shaped Resonator

The figures do depict the contours of the temperature distribution over the vibrating structure caused by the thermal-elastic coupling (Fig. 5, 7, 9, 11, 13, 15, 17, 19) as well as, the contours of von-Misses stress (Fig 6, 8, 10, 12, 14, 16, 18, 20). It could be mentioned that different modes of the investigated resonators may possess very different values of the ratio Q/f (Q-factor over modal frequency). The ratio (which has the time dimension) may be reasonably employed for the evaluation of the level of TED of differently shaped modes of resonators of different geometries, if the excitation frequency value is predetermined.

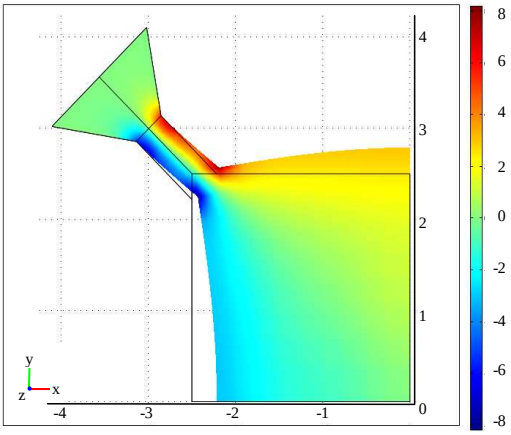

Fig. 5. Distribution of temperature at 1st in-plane quarter-symmetry modal shape of the rectangular resonator presented in Fig. 2, f= 74 743 650 Hz; Q=17 466 420, Q/f=0.2337s.

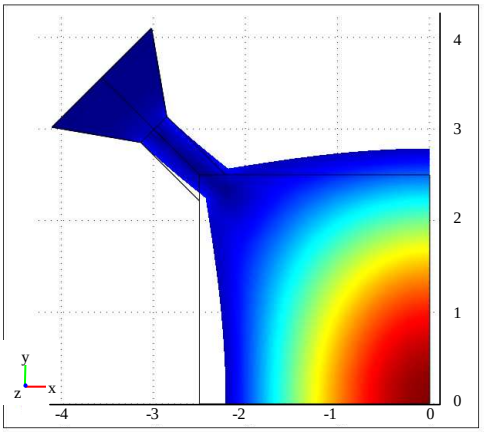

Fig. 6. Distribution of von Misses stress at 1st in-plane quarter-symmetry mode vibration of the rectangular resonator presented in Fig. 2, f= 74 743 650 Hz; Q=17 466 420, Q/f=0.2337s.

The necessary value of modal frequency can be ensured by selecting proper size of the MEMS resonator, and the ratio Q/f is independent of the resonator size as the investigated MEMS system is linear in the context of the investigated models.

The very different values of ratio Q/f of the modes, which are quite "similar" at the first sight, may be explained on the base of strained state corresponding to the modal shape. As a rule, higher TED levels possess the modes with dominating longitudinal strain components, for example, see rectangular resonators presented in Figs. 3 and 4. Shear and bending strain

dominated modes have considerably smaller TED damping ratios, see Figs.5 and 6, where the "necks" supporting the rectangular resonator on the main body of the MEMS experience mainly bending and shear strains, and the resonator is predominantly sheared. Naturally, such explanations do not pretend to be complete and exhaustive, as volumetric strained state in a solid always is quite complex and always possesses all strain components. The examples of two in-plane modes of ring resonators do not expose such noticable differences in Q/f ratio values as could be observed in the case of rectangular resonators.

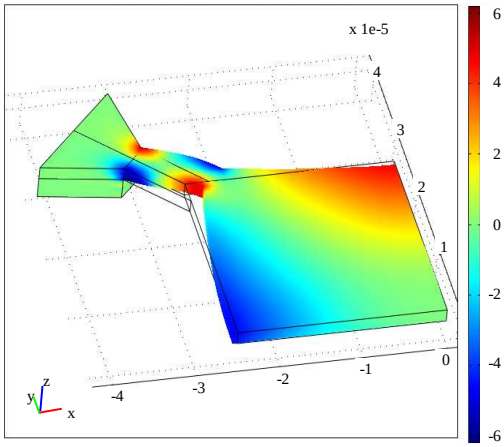

Fig. 7. Distribution of temperature at 2nd in-plane quarter-symmetry mode vibration of the rectangular resonator presented in Fig. 2,
f=86 161 050 Hz; Q= 219 606, Q/f=0.0025s.

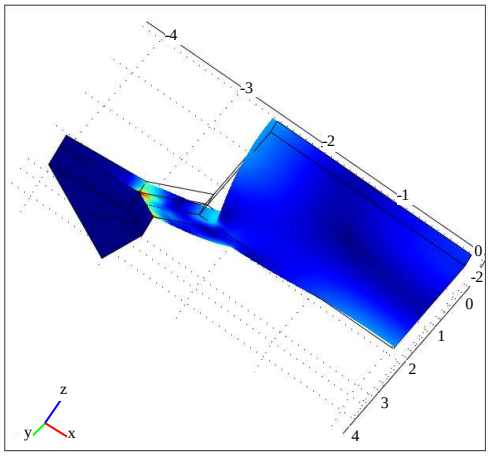

Fig. 8. Distribution of von Misses stress at 2nd in-plane quarter-symmetry mode vibration of the rectangular resonator presented in Fig. 2,
f=86 161 050 Hz; Q= 219 606, Q/f=0.0025s.

Out of plane modes are dominated by bending strains and exhibit lower values of the Q/f ratio. For the mode of the rectangular resonator presented in Figs. 9 and 10 we obtained the value such low as Q/f=0.00034s .

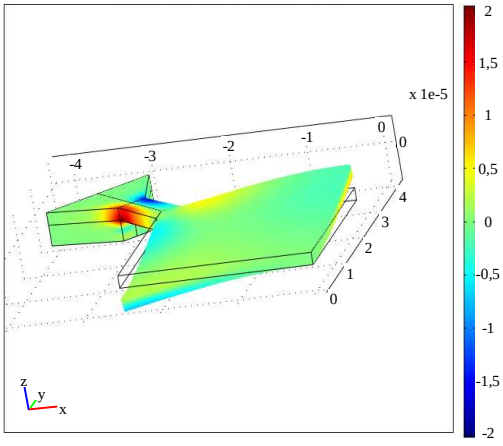

Fig. 9. Distribution of temperature at out-of-plane quarter-symmetry mode vibration of the rectangular resonator presented in Fig. 2,
f=5 573 732 Hz; Q=154 149, Q/f=0.0277s.

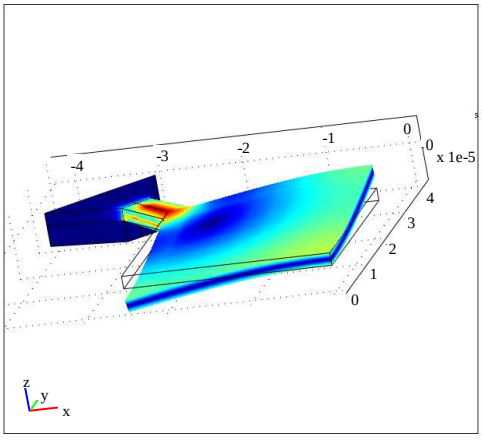

Fig. 10. Distribution of von Mises stress at out-of-plane quarter-symmetry mode vibration of the rectangular resonator presented in Fig. 2,
f=5 573 732 Hz; Q=154 149, Q/f=0.0277s.

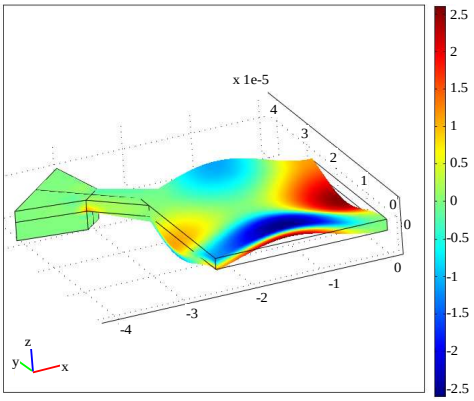

Fig. 11. Distribution of temperature at out-of-plane quarter-symmetry mode vibration of the rectangular resonator presented in Fig. 2,
f= 29 312 490 Hz; Q= 9915, Q/f=0.00034s.

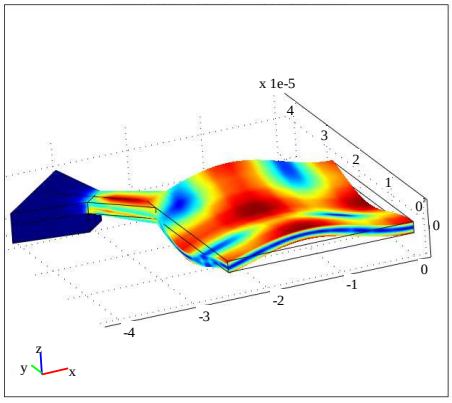

Fig. 12. Distribution of von Mises stress at out-of-plane quarter-symmetry mode vibration of the rectangular resonator presented in Fig. 2,
f= 29 312 490 Hz; Q= 9915, Q/f=0.00034s.

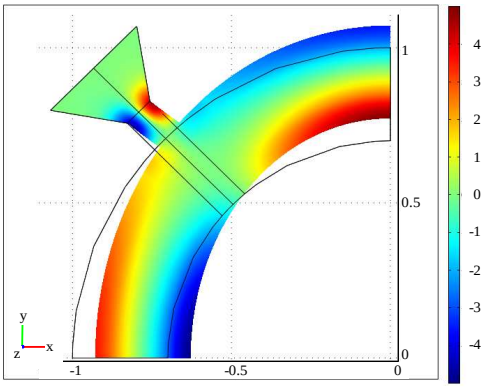

Fig. 13. Distribution of temperature at 2nd in plane quarter-symmetry mode vibration of the ring resonator presented in Fig. 4,
f= 4 456 137 Hz; Q=75793, Q/f=0.017s.

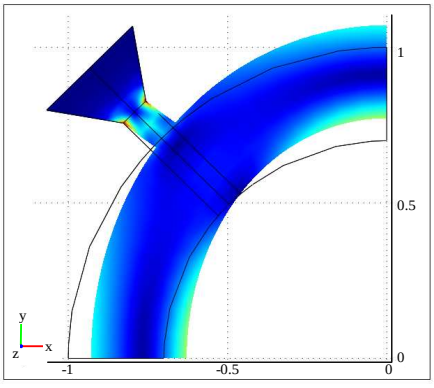

Fig. 14. Distribution of vonMisses stress at 1st in-plane quarter-symmetry mode vibration of the ring resonator presented in Fig. 4,
f= 4 456 137 Hz; Q=75793, Q/f=0.017s.

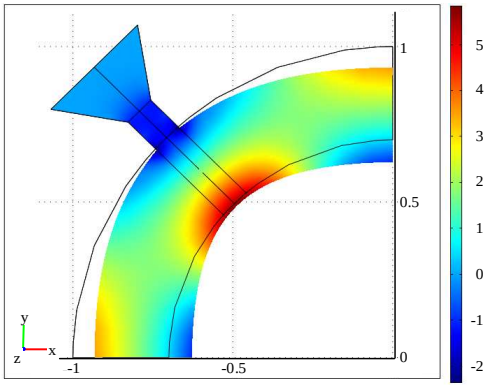

Fig. 15. Distribution of temperature at 2nd in-plane quarter-symmetry mode vibration of the ring resonator presented in Fig. 4,
f= 17 078 160 Hz; Q= 1 078 869, Q/f=0.0632s.

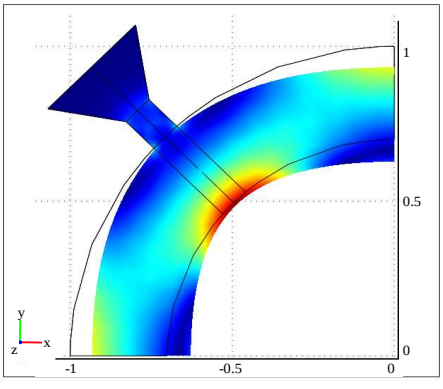

Fig. 16. Distribution of vonMisses stress at 2nd in-plane quarter-symmetry mode vibration of the ring resonator presented in Fig. 4,
f= 17 078 160 Hz; Q= 1 078 869, Q/f=0.0632s.

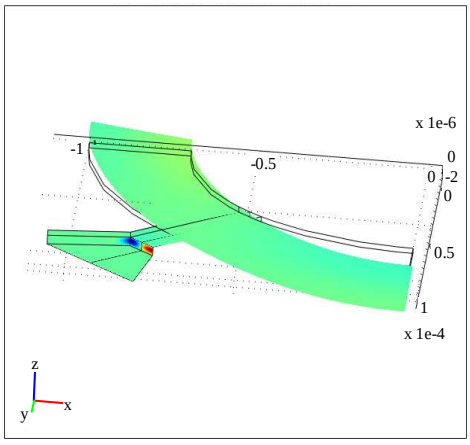

Fig. 17. Distribution of temperature at out-of-plane quarter-symmetry mode vibration of the ring resonator presented in Fig. 4,
f= 362 032 Hz; Q= 2582, Q/f=0.0071s.

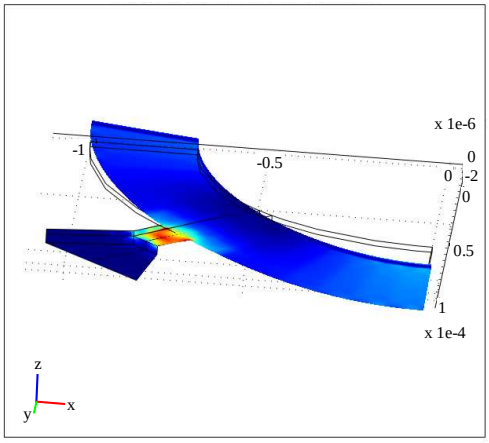

Fig. 18. Distribution of temperature at out-of-plane quarter-symmetry mode vibration of the ring resonator presented in Fig. 4,
f= 362 032 Hz; Q= 2582, Q/f=0.0071s.

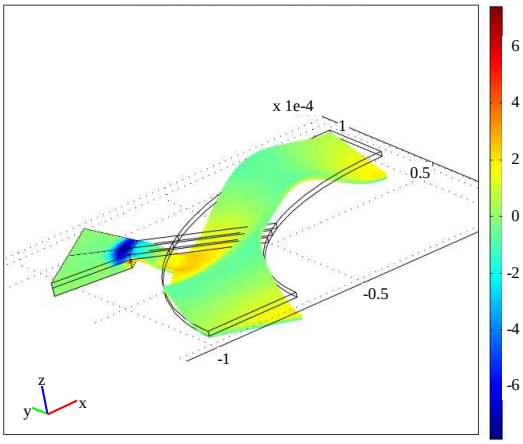

Fig. 19. Distribution of temperature at out-of-plane quarter-symmetry mode vibration of the ring resonator presented in Fig. 4,
f= 6 610 465 Hz; Q= 47296, Q/f=0.0072s

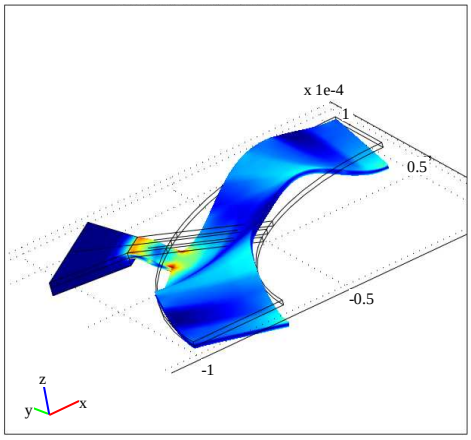

Fig. 20. Distribution of vonMises stress at out-of-plane quarter-symmetry mode vibration of the ring resonator presented in Fig. 4,
f= 6 610 465 Hz; Q= 47296, Q/f=0.0072s.

Model verification and validation

A significant part of any simulation is the verification and validation of the model. It is necessary to be sure that the model design (conceptual model) is transformed into a computer model with sufficient level of adequacy and accuracy.

In this study, a sample model of a cantilever beam resonator (Fig. 21) has been investigated numerically and experimentally. Three modifications of the sample cantilever resonator numerical model have been explored:

a. real clamping conditions and the presence of the SiO_2 substrate taken into account as in Fig. 21. Full clamping and prescribed temperature (ambient temperature T_0) boundary conditions imposed for all cut-boundaries that separate the computational model form the remaining body of the MEMS. The model houses the resonating structure and a part of the surrounding domain. The mechanically free surfaces of the model are assumed to be thermally isolated;
b. the cantilever resonator presented without the surrounding material. One end of the resonator is fully clamped, and fixed temperature boundary conditions imposed at this end;
c. The same model as in (b), with the clamped end thermally isolated.

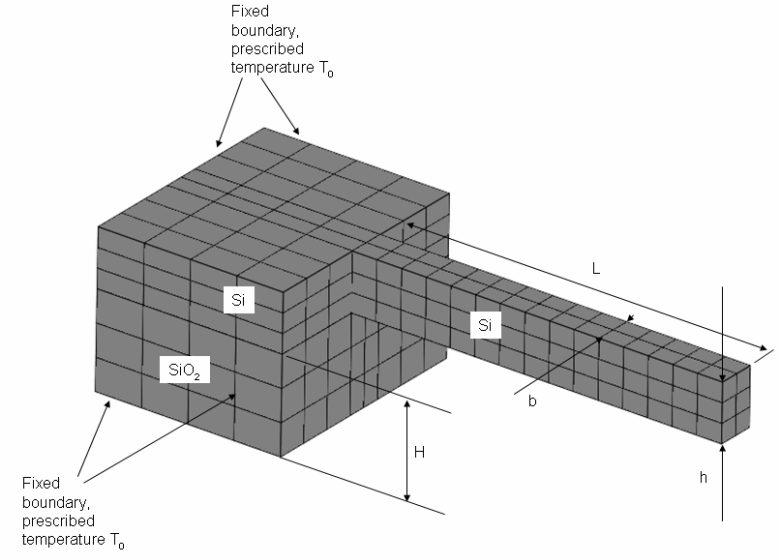

Fig. 21. Geometry and finite element discretization of the sample model of cantilever beam resonator,

$$b = 1\times10^{-6}m;\quad h = 1.5\times10^{-6}m;\quad H = 2.5\times10^{-6}m$$

Table 1 presents the first modal frequency and Q-factor values of the three models of the Poly-Si cantilever resonator at three different values of its length. Model modification (a) is close to the situations observed in a real MEMS. However, analytical formulae are able to evaluate the situations b and c only, therefore they are used for comparisson of the results and model verification.

Table 1. Modal frequency and Q-factor values of the sample cantilever resonator

Resonator length L (m)	Model modification a	Model modification b	Model modification c
$L = 0.5\times10^{-5}$	$f = 48.12MHz;$	$f = 54.3MHz;$	$f = 54.3MHz;$
	$Q = 1.347\times10^{4}$	$Q = 1.472\times10^{4}$	$Q = 1.074\times10^{4}$
$L = 1\times10^{-5}$	$f = 13MHz;$	$f = 13.8MHz;$	$f = 13.8MHz;$
	$Q = 4.13\times10^{4}$	$Q = 4.6\times10^{4}$	$Q = 4.6\times10^{4}$
$L = 2\times10^{-5}$	$f = 3.358MHz;$	$f = 3.46MHz;$	$f = 3.46MHz;$
	$Q = 1.612\times10^{5}$	$Q = 1.736\times10^{5}$	$Q = 1.549\times10^{5}$

The thermal boundary conditions influence the TED effects (i.e., the Q-factor values). Ideally clamped resonator models as in modifications (b) and (c) produce increased natural frequency values compared with more adequate model (a).

Fig. 22 demonstrates the comparisson of the first modal frequency and Q-factor values obtained by using FE models against analytical evaluations. The model parameters have been matched to the design data of poly-Si and poly-C resonators given in [6]. The resonators were fabricated and tested by using piezoelectric and electrostatic actuation methods in low and high vacuum.

Fig. 22, presents the dependencies of the Q-factor values determined by different vibration energy loss mechanisms against the resonant frequencies of poly-Si and poly-C 1μm thick cantilever beam resonators.

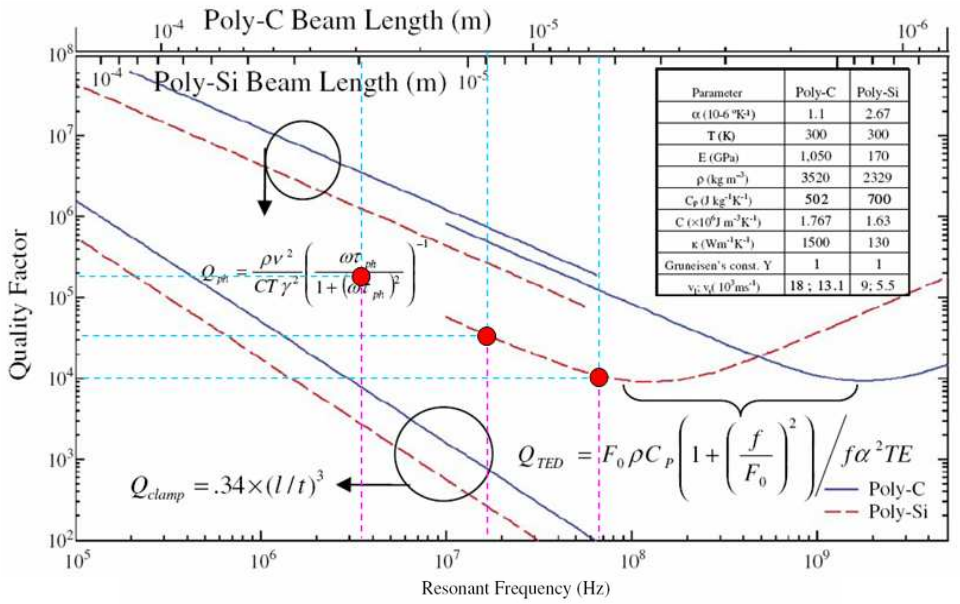

Fig. 22. Dependencies of Q-factor values determined by different vibration energy loss mechanisms against the resonant frequencies of poly-Si and poly-C cantilever resonators, [6]. Red dots indicate the numerical results obtained in this work by FE analysis for Poly-Si cantilever resonators of length $9 \cdot 10^{-4}$ m; $2 \cdot 10^{-5}$ m, and $6{,}5 \cdot 10^{-5}$ m

The simulation results have been validated experimentally. Series of two types of structures on the wafer – cantelivers and double-clamped beam resonators square- and ring-shaped ones – were designed and manufactured for experimental characterisation. The resonator structure used in this study was a cantilever beam of length 60 μm and width 6 μm. The gap between resonators and electrodes is around 700 nm (designed). The excitation and readout mechanism was capacitive.

The dependence of the numerically obtained values of the Q-factor of 1st damped mode against temperature is depicted in Fig. 23.

The measurements for the validation purposes were performed at the MEMS testing laboratory at the Interuniversity Microelectronics Center (IMEC). The aim of the experiments was obtaining information concerning the effect of temperature on both the modal frequency and Q-factor. The resonator was tested in the vacuum set-up over the range of reference temperatures and bias voltages. The pressure in the vacuum chamber was kept constant at a

pressure of 1.6·e-4 mbar. In the experiments conducted the temperature was varied between -30°C and 120°C in steps of 5 K.

The resonance frequency and the Q-factor values were extracted from the recorded data, and the Q-factor/resonance frequency dependency on temperature was developed. The results of the extraction procedure are presented in Fig. 24. It can be admitted that the qualitative agreement of numerical and experimental results is good (about 2500 drop of the Q-factor value over temperature range of 100°C in both cases). However, the experimentally obtained Q-factor value is about 2700 higher over all temperature range. It seems reasonable to conclude that the difference of values is caused by other damping mechanisms not represented by purely TED model. Simultaneously, the obtained values proove the major signifficance of TED during vibrations of MEMS resonators, as the value of the Q-factor caused by TED is approximately 8000-10500 against 5500-8000, which is obtained if simultaneously other energy dissipation mechanisms are taken into account.

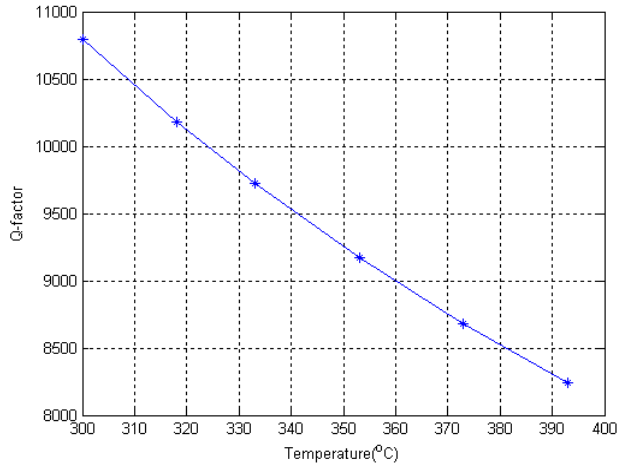

Fig. 23. The dependence of numerically obtained values of the Q-factor of the 1st damped mode against temperature

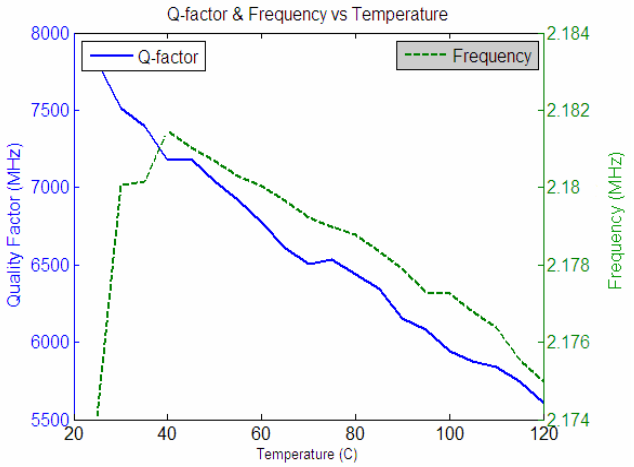

Fig. 24. The experimentally obtained dependence of the 1st damped modal frequency and Q-factor against temperature

Experimental studies focusing on energy loss mechanisms concerned are under way and will be the subject of subsequent publications.

Conclusion

The finite element modelling of thermoelastic modal damping (TED) of MEMS vibrations developed in [3] has been extended and applied to the analysis of rectangular- and ring-shaped resonators. The sample models have been verified by peroforming comparissons against analytical calculations and by corresponding experimental investigations. The comparison of calculated and experimentally obtained resonant frequencies and Q-factor values indicated a good agreement of tendencies of change of the quantities against temperature. Both the experimentsand calculations revealed an almost linear decrease of the Q-factor against temperature. However, all experimental Q- factor values were lower than theoretical ones. The shift of the values could be explained by other mechanisms of damping, which are not included into the thermal-elastic damping model. Their influence can be quantitatively evaluated by the said difference of the values.

Acknowledgement

The research is sponsored by NATO RTO and Lithuanian State Science and Studies Foundation.

References

[1] **Cornelius T. Leondes**, Ed., MEMS/NEMS Handbook: Techniques and Applications, Vol. 1-5, Springer Science, 2006.

[2] **Wise K. D., Najafi K.**, The Engineering Research Center for Wireless Integrated MicroSystems (WIMS) *Annual Report 2007*, University of Michigan, Michigan State University, Michigan Technological University, http://www.wimserc.org.

[3] **Barauskas R., Kausinis, S., De Wolf I., Stoffels S., Tilmans H. A. C.,** Finite element analysis of thermo-elastical modal damping of MEMS vibrations // Journal of Vibroengineering / Vibromechanika, Lithuanian Academy of Sciences, Kaunas University of Technology, Vilnius Gediminas Technical University. ISSN 1392-8716. 2007, Vol. 9, no. 2. p. 21-33.

[4] **Zhang W., Kimberly L. Turner**, Thermoelastic Damping in the Longitudinal Vibration: Analysis and Simulation, Proceedings of IMECE04, 2004 ASME International Mechanical Engineering Congress and Exposition, November 13-20, 2004, Anaheim, California USA.

[5] **Mohanty P., Harrington D. A., Ekinci K. L., Yang Y. T., Murphy M. J., and Roukes M. L.** Intrinsic dissipation in high-frequency micromechanical resonators, PHYSICAL REVIEW B 66, 085416, 2002.

[6] **Sepulveda N., Aslam D., Sullivan J.P.**, Polycrystalline diamond MEMS resonator technology for sensor applications, Diamond & Related Materials 15 (2006) 398 – 403

[7] **Harrington D. A., Mohanty P., Roukes M. L.**, Energy dissipation in suspended micromechanical resonators at low temperatures, Physica B 284}288 (2000) 2145-2146

[8] **Ekinci K. L., Roukes M. L.,** Nanoelectromechanical systems, Review of Scientific Instruments, 76, 061101 (2005)

[9] **Feng X. L., Zorman C. A., Mehregany M., and Roukes M. L.**, Dissipation in Single-Crystal 3C-SIC Ultra-High Frequency Nanomechanical Resonators, Tech. Digest, Solid-State Sensors, Actuators, and Microsystems Workshop (Hilton Head 2006), pp. 86-89.

[10] **Clarence Zener**, *Physical Review.V52-53,(1937-1938).*